

# Marangoni flow of molten silicon: The effects of oxygen partial pressure

T. HIBIYA

Department of Aerospace Engineering, Tokyo Metropolitan Institute of Technology, 6-6, Asahigaoka, Hino 191-0065, Japan

Instability of the Marangoni flow of molten silicon is discussed. Time-dependent behavior of azimuthal wave numbers ( $m$ ) for flow instability was investigated based on temperature oscillation measurements using a  $\theta$ - $t$  analysis, and appearance ratio of each azimuthal wave number is analyzed. The relationship between frequency and azimuthal wave numbers is deduced from an analysis of appearance ratios at a decomposed frequency band using a wavelet analysis. Oxygen partial pressure at the melt surface can be predicted using the Ratto-Ricci-Arato model. Anomalous recalescence behavior and surface oxidation of levitated molten silicon are shown. Growth striation is induced in silicon crystals grown even under high oxygen-partial pressure. © 2005 Springer Science + Business Media, Inc.

## 1. Introduction

The Marangoni flow of a molten semiconductor is one of the typical features of high temperature capillarity. The existence of Marangoni flow in a silicon melt was experimentally confirmed for the first time through crystal growth experiments under microgravity [1]. In order to simulate the Marangoni flow in floating zone crystal growth and to simplify the phenomena to be observed, a half-zone configuration has been employed [2]. Experimental research on Marangoni flow of low  $Pr$  (Prandtl number) fluids such as molten metals and semiconductors has been difficult due to the characteristics of these melts, i.e., high temperature, oxidation of the melt surface and opaqueness to the visible light. Marangoni flow shows instability; it changes from an axisymmetric stationary flow to three-dimensional stationary flow, and then to oscillatory flow. A critical Marangoni number for conversion of the flow mode from a stationary to an oscillatory flow mode is small for low  $Pr$  fluids [3]. However, since it is difficult to generate experimentally small Marangoni numbers for low  $Pr$  fluids [4], experimental approaches have been carried out in the high Marangoni number ranges, i.e.  $Ma \approx 10^3$ – $10^4$ . The Marangoni number  $Ma$  is defined as follows,

$$Ma = \frac{(-\partial\sigma/\partial T) \cdot \Delta T \cdot h}{\mu \cdot \kappa}, \quad (1)$$

Where  $\partial\sigma/\partial T$  is the temperature coefficient of the surface tension,  $\mu$  and  $\kappa$  are viscosity and thermal diffusivity, respectively.  $\Delta T$  is the temperature difference and  $h$  is the characteristic length of the system defined as height of the bridge.

On the other hand, numerical research has been concentrated on the low Marangoni number, i.e.  $Ma \approx 10^2$ . Research has been carried out to observe flow mode conversion from axisymmetric stationary flow

to three-dimensional stationary flow and from three dimensional stationary flow to oscillatory flow [5–8]. Thus, the Marangoni number used for numerical modeling has been lower one just above the second critical number,  $Ma_{c2}$ , where the stationary flow changes to oscillatory flow. The relationship between the aspect ratio ( $As$ ) and the wave number ( $m$ ) of flow instability has been clarified, as follows,

$$As \cdot m = 2 \sim 2.2 \quad (2)$$

In this Marangoni number range, Imaishi *et al.* reported that evolution of flow instability takes place as time passes [8, 9].

In experimental approaches to this topic, temperature- and flow-fields have been observed by measuring temperature oscillation using thermocouples [2] and a fiber sensor [10], and by observing flow using X-ray radiography with tracer particles [11]. Crystal growth and observation of growth striation are important methods for correlating instability of the Marangoni flow with qualities of the crystals [12, 13]. The Marangoni flow study at high Marangoni number ranges (such as 1000–10000) is important from the crystal growth viewpoint, since the Marangoni flow during floating-zone crystal growth has such high Marangoni numbers, i.e. almost chaotic.

The flow structure at high Marangoni numbers has not yet been clarified either experimentally or numerically, although Nakamura *et al.* analyzed the frequency of temperature oscillations using a FFT (fast Fourier transformation) technique. They experimentally confirmed the formation of a non-axisymmetric temperature field and its oscillation through analyzing the phase relationship of temperature oscillation and flow visualization using X-ray and tracer particles [2, 14]. However, frequencies of corresponding wave numbers, dependence of frequency on aspect ratio and

time evolution of mode structures have not been clarified. As long as the FFT technique is employed, it is difficult to extract time-dependent data in the long range.

Another important feature of the Marangoni flow for a low  $Pr$  fluid, such as molten silicon, is the effect of oxygen partial pressure. For the Marangoni flow of molten silicon, it has been found that the velocity of the flow and the temperature oscillation mode are dependent upon the oxygen partial pressure of an ambient atmosphere [15, 16]. The amplitude of the melt/solid interface oscillation has also indicated effects caused by oxygen partial pressure [17]. The effects of oxygen partial pressure on the temperature coefficient of the surface tension were capable of explaining these phenomena, because the temperature coefficient of the surface tension is a driving force of the Marangoni flow [18]. However, the oxygen partial pressure range measured in Marangoni flow experiments and in the case of surface tension measurements show very large differences, exceeding ten orders of magnitude. Although they must be the same, they exhibit very large differences. Because physicochemical phenomena take place at the melt surface, it has been necessary to know the oxygen partial pressures at the melt surface. However, experimentally it is almost impossible to measure oxygen partial pressures at the melt surface; in the case of Azami's (Marangoni flow) [15], the oxygen partial pressure was measured when the quartz ampoule was sealed, whereas for Mukai's (surface tension measurement) experiments, [18], it was measured at the exit of the gas flow system. Thus, it is necessary to estimate the oxygen partial pressure at the melt surface either from that measured at the inlet or at the exit of the gas flow system. According to Ratto and his coworkers, there is big difference in oxygen partial pressure depending on the measurement location; measurements tend to show high oxygen partial pressures at the inlet of the system, whereas they tend to be lower at the exit of the system [19]. This is due to the fact that the system contains volatile oxides [20]. Taking into account the chemical equilibrium at the melt gas interface and transport of oxygen from and to the melt surface, Ratto and his coworkers presented a model to estimate oxygen partial pressure at the melt surface. This can be done either through measuring oxygen partial pressure at the inlet of the system or through measuring it at the exit of the system, as follows [19],

$$P_{O_2}^{\text{inlet}} = P_{O_2}^{\text{surface}} + P_{Si}^{\text{saturation}} \sum_{j=1}^2 \alpha_j K_j \times \frac{(1 + Pe)}{(1 + Pe/|\psi_j|)} P_{O_2}^{\text{surface}\alpha_j} \quad (3)$$

$$P_{O_2}^{\text{exit}} = P_{O_2}^{\text{surface}} + P_{Si}^{\text{saturation}} \sum_{j=1}^2 \alpha_j K_j \times \frac{(Pe)}{(1 + Pe/|\psi_j|)} P_{O_2}^{\text{surface}\alpha_j} \quad (4)$$



for  $j = 1$ ,  $Si(l) + 1/2 O_2(g) \rightarrow SiO(g)$  and  $\alpha_1 = 1/2$ , and for  $j = 2$ ,  $Si(l) + O_2(g) \rightarrow SiO_2(s)$  and  $\alpha_2 = 1$ .

Here,  $K_j$  is the dimensionless equilibrium constant for the  $j$ th reaction,  $\Psi_j$  is the dimensionless diffusion constant of oxygen, and  $Pe$ , the Peclet number, is defined as the ratio of flow to diffusion of oxygen. In order to check if this model is valid or not, simultaneous measurements of oxygen partial pressure both at the inlet and exit of the system are required.

As a result of the determination of the influence of oxygen partial pressure on the surface tension of molten silicon by Mukai *et al.* [18], it is suggested that the surface tension of molten silicon in an oxygen-supersaturated environment can be measured, if a containerless technique is employed to avoid nucleation of the  $SiO_2$  phase. This is a metastable surface tension with respect to oxygen.

In the present paper, the time evolution of the Marangoni flow instability is discussed. Frequency bands for the azimuthal wave numbers,  $m = 1$  and  $m = 3$ , are determined and the aspect ratio ( $As$ ) dependence of frequency is discussed. The Ratto model, which can show the oxygen partial of melt surface, regardless of measurement locations, i.e., inlet or exit, is experimentally validated. Also, the possibility of the measuring surface tension of molten silicon under supersaturated oxygen condition is discussed. Crystal growth was attempted in an atmosphere with various oxygen partial pressure conditions to observe the effect of oxygen partial pressure on growth striation introduced by oscillatory Marangoni flow.

## 2. Experimental setup

Figs. 1a–c show a setup for the Marangoni flow experiment. A molten silicon bridge was prepared between the upper and the lower carbon shafts within a mono-ellipsoidal infrared furnace, so that a unidirectional temperature gradient was attained from the top to the bottom of the bridge. We measured temperature oscillation using six  $R$ -type thermocouples, which were set  $60^\circ$ -apart from each other azimuthally in the liquid bridge close to the cold shaft. Temperature oscillation data were analyzed by using a  $\theta$ - $t$  plot of the temperature oscillations of six thermocouples and a wavelet transformation using the spline-4 function [21]. Deformation and oscillation of the liquid bridge surface due to flow instability was observed by a phase shift interferometry combined with a wavelet transformation using the Gabor function, so that the time dependence of the oscillation could be analyzed [22].

In order to validate Ratto's model, the oxygen partial pressure was measured simultaneously at the inlet and the exit of the gas flow system changing gas flow rate, as shown in Fig. 2 [23]. In order to observe the surface behavior of silicon melt with respect to oxygen partial pressure, the surface of electromagnetically-levitated molten silicon was observed in an ambient atmosphere with various oxygen partial pressures and various temperatures; oxygen partial pressures including super-saturation conditions and temperature ranges including undercooled conditions [24].

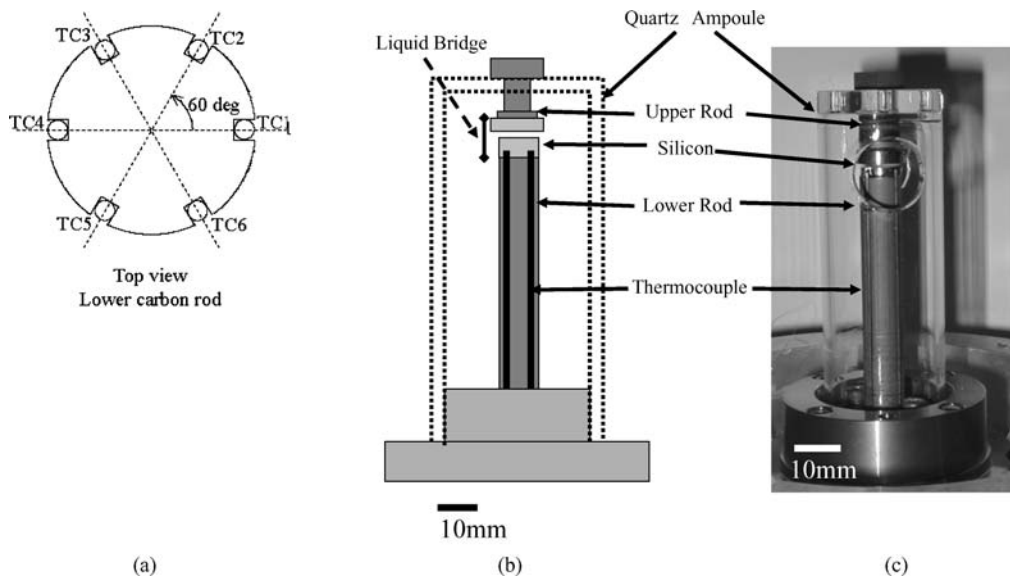


Figure 1 Configuration of sample. (a) Layout of thermocouples (top view), (b) side view and (c) photograph.

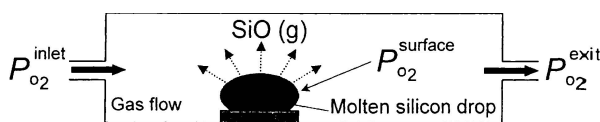


Figure 2 Silicon droplet in gas flow condition.

Silicon single crystals were prepared by a floating zone technique using an infrared mirror furnace. Growth striation was observed using NDIC (Nomarski differential interference contrast) microscopy [13].

### 3. Results and discussion

#### 3.1. Time dependent behavior of flow instability

Fig. 3a and b show azimuthal distributions for a non-axisymmetric temperature field and its time dependence for a molten silicon bridge with an aspect ratio of  $As = 2.0$  and Marangoni number of  $Ma \approx 14000$ . Details of the method used to obtain temperature field are explained in ref. [21]. Temperature oscillation data obtained by six thermocouples were interpolated along the azimuthal direction using a cubic spline function to indicate symmetry and oscillation of the temperature field visually. Fig. 3a shows a snapshot of the azimuthal dis-

tribution of a temperature field at 7.5s of the  $\theta-t$  plot of oscillation of the temperature field (Fig. 3b). Note that information along the radial direction has no meaning in Fig. 3a. As shown in Fig. 3a and b, azimuthal temperature distribution shows almost one-fold symmetry; i.e. the azimuthal wave number  $m = 1$ . It is clear that the one-fold symmetric temperature field starts to rotate three seconds after the start of observation, as shown in Fig. 3b. Before that two fold symmetry ( $m = 2$ ) is likely to exist. However, when the  $m = 1$  mode was observed using four thermocouples under microgravity conditions [2], rotation was not observed. Through the  $\theta-t$  plot analysis, the three-fold symmetric temperature field was observed; this was impossible when four thermocouples were used. Formation of non-axisymmetric temperature fields with  $m$ -fold symmetry is explained by Wanschura *et al.* [6]. It is noteworthy that the relationship between the azimuthal wave number and the aspect ratio is valid even with such a high Marangoni numbers, where flow is almost turbulent. The existence of a basic structure even at high Marangoni numbers was also confirmed by decomposing the temperature oscillation data using a wavelet transformation analysis and the spline-4 function. For example, the frequency observed in the present study of  $f = 0.08-0.2$  Hz for the  $As = 2.0$  case agrees with that for  $f = 0.2$  Hz for

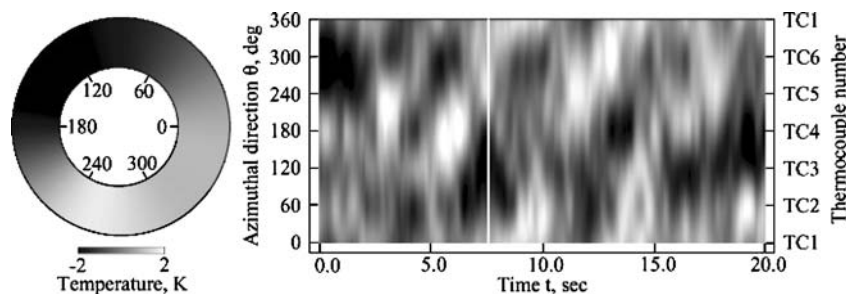


Figure 3 The  $\theta-t$  analysis of temperature oscillation showing time evolution of azimuthal distribution of non-axisymmetric temperature field for the liquid bridge with an aspect ratio of  $As = 2.0$  and Marangoni number of  $Ma = 14000$ . One-fold symmetric temperature field ( $m = 1$ ) rotates.

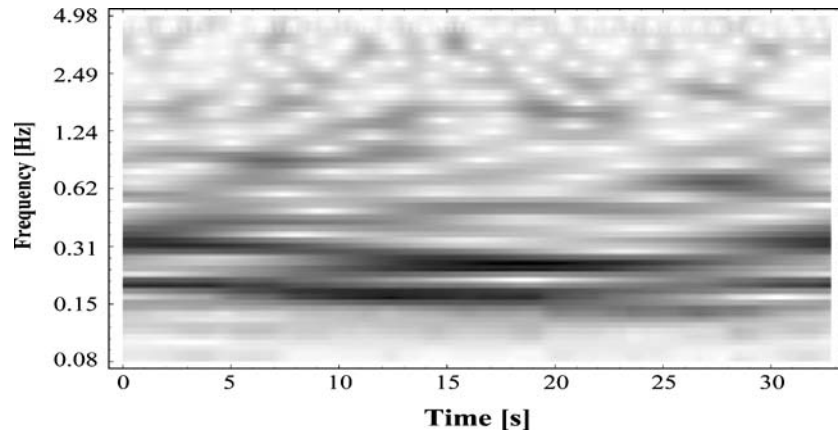


Figure 4 Frequency plane obtained by a wavelet transformation analysis using a Gabor function for the liquid bridge with an aspect ratio of  $As = 1.0$  and estimated Marangoni number of  $Ma = 5000$ .

the  $As = 2.0$  case using a FFT technique [2]. Further discussion of this point can be found elsewhere [21].

Fig. 4 shows an example of a wavelet transformation analysis for surface oscillation of the liquid bridge using phase-shift interferometry. This shows a frequency-time relationship (a frequency plane) of oscillation of the azimuthal gradient of the bridge with an aspect ratio of  $As = 1.0$  and an estimated Marangoni number of  $Ma \approx 5000$ . Because surface oscillation was observed using a combination of FFT and wavelet transformation analyses, it was possible to confirm that two frequency bands are likely to exist. The lower frequency band appeared during entire observation period and its frequency ranged from 0.1 to 0.5 Hz. The higher frequency band appeared intermittently and the central frequency ranged from 0.5 to 1.2 Hz. Since the frequencies for the  $m = 1$  and  $m = 3$  modes were estimated to be 0.08–0.2 Hz and 0.01–0.2 Hz, respectively, from the frequency band analysis [21], the higher frequency band, which ranged from 0.5 to 1.2 Hz, could be interpreted to be specific to the  $m = 2$  mode, although the frequency band analysis cannot predict the frequency for the  $m = 2$  mode [21], because higher azimuthal wave numbers such as  $m = 4$  can be identified as  $m = 2$  whenever six thermocouples are used. Further discussion on this point can be found elsewhere [22].

### 3.2. Oxygen partial pressure at the Simelt surface

In order to observe whether Ratto’s model is valid, oxygen partial pressures were measured using the gas flow conditions at both the inlet and exit of the system (see Fig. 2):  $P_{O_2}^{inlet}$  and  $P_{O_2}^{exit}$ . As shown in Fig. 5,  $P_{O_2}^{inlet}$  and  $P_{O_2}^{exit}$  show differences, and  $P_{O_2}^{exit}$  depends on the flow rate of mixed gas (0.5 to 5.0 l·min<sup>-1</sup>), even though  $P_{O_2}^{inlet}$  was fixed at  $1.1 \times 10^{-1}$  Pa.  $P_{O_2}^{exit}$  was also measured as a function of the  $P_{O_2}^{inlet}$  at a constant flow rate of mixed gas (3.0 l·min<sup>-1</sup>) (see Fig. 6). Although the  $P_{O_2}^{exit}$  depends on the  $P_{O_2}^{inlet}$ , the  $P_{O_2}^{exit}$  and  $P_{O_2}^{inlet}$  are almost the same when the  $P_{O_2}^{inlet}$  was  $7.5 \times 10^2$  Pa (and  $P_{O_2}^{exit}$  was  $4.8 \times 10^2$  Pa). This means that under these conditions, the silicon melt surface became coated with a SiO<sub>2</sub> film and no more oxygen gas could react with the molten silicon. This  $P_{O_2}^{inlet}$  of  $7.5 \times 10^2$  Pa almost corresponds to the oxygen partial pressure for saturation, defined at the inlet, which corresponds to the  $P_{O_2}^{surface}$  of  $2.8 \times 10^{-14}$  Pa, as shown in Fig. 7. This figure was plotted by substituting the above experimental results into Equation 3 and this shows the relationships between  $P_{O_2}^{surface}$  and  $P_{O_2}^{inlet}$ . It is clear that a  $P_{O_2}^{surface}$  of  $2.8 \times 10^{-14}$  Pa is of the same order of magnitude as the theoretical oxygen partial pressure for saturation at 1688 K, i.e.,  $P_{O_2}^{saturation}$  of  $1.1 \times 10^{-14}$  Pa, and also  $P_{O_2}$

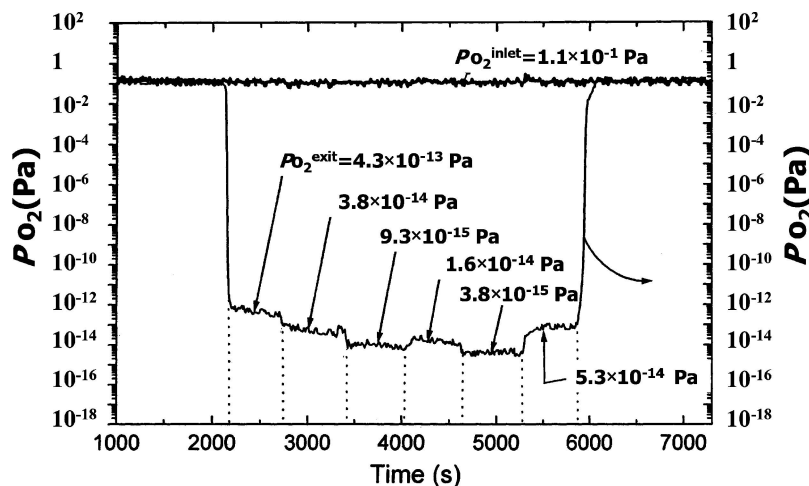


Figure 5 The effect of the flow rate of inlet gas on the oxygen partial pressure measured at the exit [23].

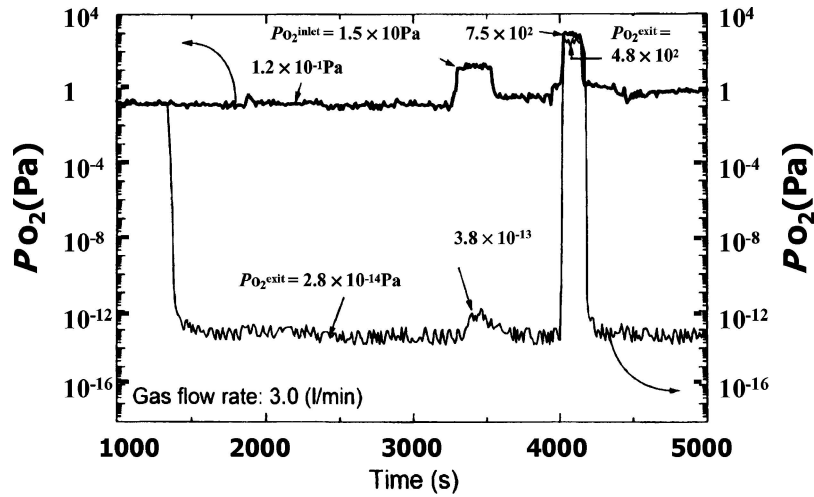


Figure 6 Relationship between oxygen partial pressures measured at the inlet and at the exit of the furnace for constant flow rate of mixed gas (3.0 l·min<sup>-1</sup>) [23].

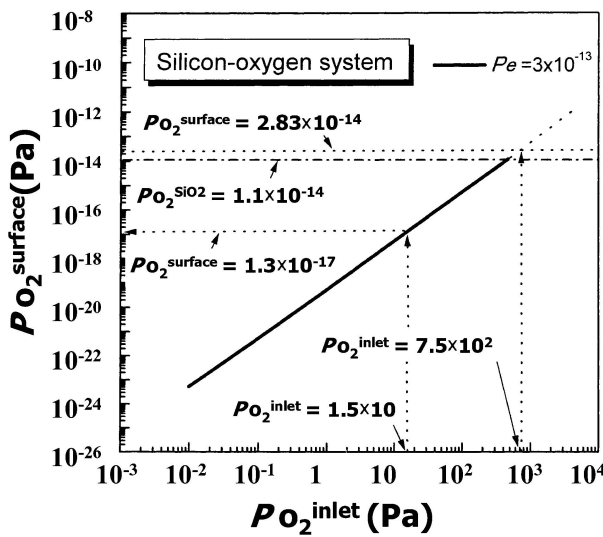


Figure 7 The relationship between the  $P_{O_2}^{surface}$  and the  $P_{O_2}^{inlet}$  [23].

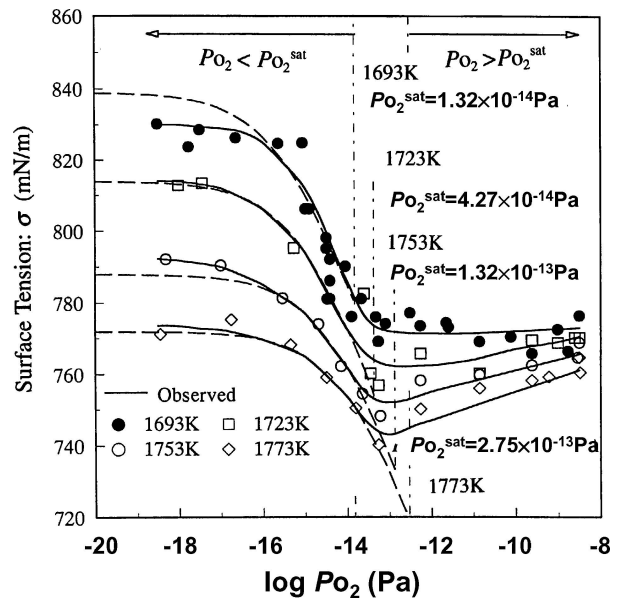


Figure 8 Surface tension of molten silicon as a function of oxygen partial pressure for various temperatures [18].

corresponds to the kink in the surface tension values measured by Mukai *et al.* as a function of oxygen partial pressure (Fig. 8). In the case of the surface tension measurements by Mukai *et al.*,  $P_{O_2}$  was measured at the exit of the furnace. Because the gas flow rate was 160 ml·m<sup>-1</sup>,  $P_{O_2}^{surface}$  can be estimated to be almost that of the  $P_{O_2}^{exit}$ . Through the simultaneous measurements of  $P_{O_2}^{inlet}$  and  $P_{O_2}^{exit}$ , Ratto's model was validated as an estimate for  $P_{O_2}^{surface}$  either from  $P_{O_2}^{inlet}$  or  $P_{O_2}^{exit}$ .

### 3.3. Surface oxidation of molten silicon

As shown in Fig. 8, oxygen partial pressure dependence of surface tension exhibits marked difference above and below the equilibrium oxygen partial pressure for formation of SiO<sub>2</sub> phase,  $P_{O_2}^{SiO_2}$ . Above the  $P_{O_2}^{SiO_2}$ , SiO<sub>2</sub> films are formed on the surface of a silicon droplet sustained on the substrate. A solid state substrate could have played a role as a nucleation site for a SiO<sub>2</sub> phase formation. Thus, if a silicon droplet is levitated using a containerless technique, the nucleation of the SiO<sub>2</sub> phase can be suppressed and then supersaturation of

the oxygen can be realized. In such a condition, the surface tension value is on the extrapolated line of surface tension from the region of  $P_{O_2} < P_{O_2}^{SiO_2}$ . This is another metastable condition in addition to undercooling, because the system is univariant for the chemical reaction of Si (liquid) + O<sub>2</sub> (gas) = SiO<sub>2</sub> (solid) and  $P_{O_2}$  is also a parameter to describe a chemical equilibrium. In order to determine the above mentioned possibility, a silicon droplet was electromagnetically levitated using combinations of various temperatures and oxygen partial pressures. A mixture of 6N-Ar and 3%O<sub>2</sub>-Ar was flowed through a quartz tube that was inserted in a levitation coil, in which a silicon droplet was levitated, as shown in Fig. 9. Employing this configuration, Ratto's required conditions were satisfied so that  $P_{O_2}^{surface}$  was controlled by changing the  $P_{O_2}^{inlet}$  of the gas flow system.

Fig. 10 shows formation of a SiO<sub>2</sub> phase at the silicon melt surface at 1620K and at  $P_{O_2}^{surface} = 3.5 \times 10^{-14}$  Pa. The SiO<sub>2</sub> phase formation does not cause solidification

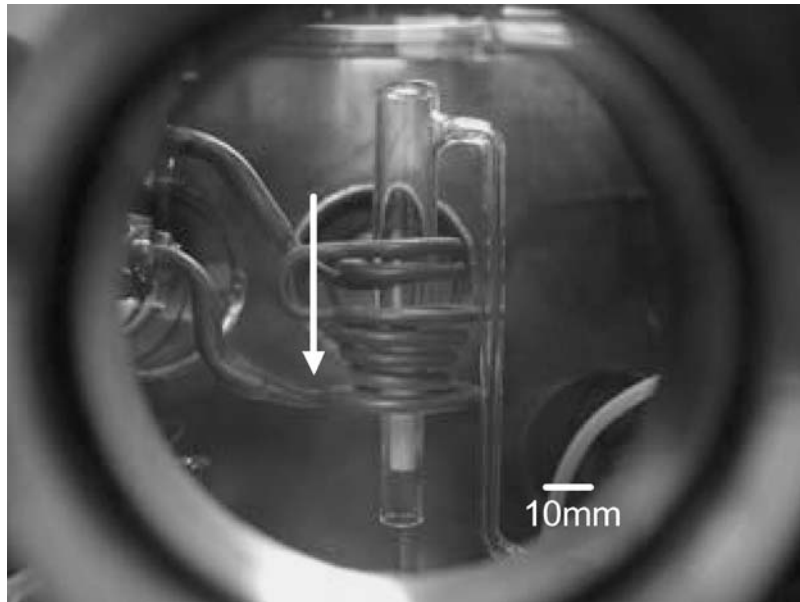


Figure 9 Quartz glass tube installed within a levitation coil; oxygen partial pressure of molten silicon at the melt surface can be controlled. An arrow shows gas flow direction.

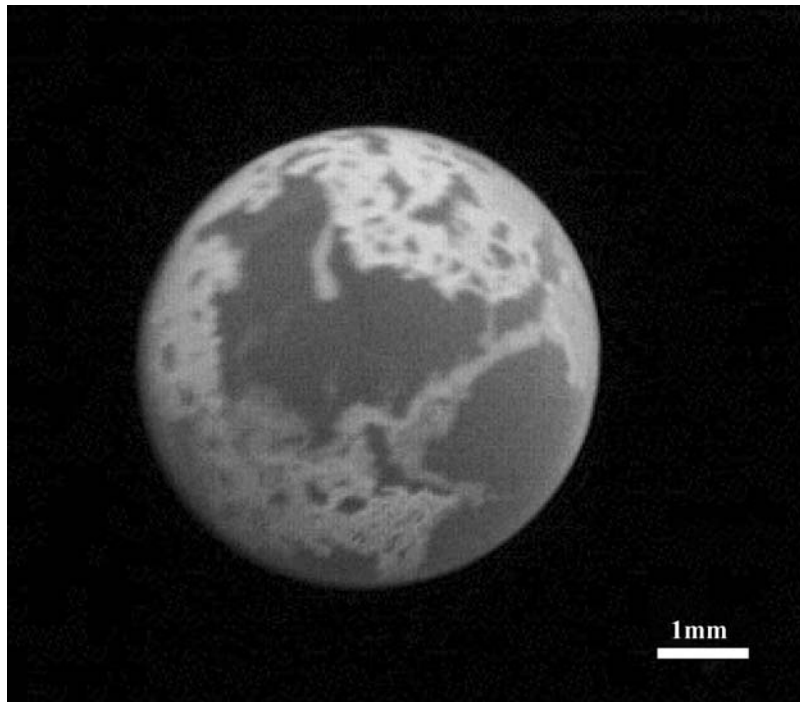


Figure 10 Formation of an oxide film on the levitated silicon surface.

of a Si phase. After the surface of the silicon melt was coated with a  $\text{SiO}_2$  film completely, the temperature of the levitated silicon droplet drops spontaneously (without control) with temperature oscillation. The observed phenomenon can be explained as follows. When the temperature of the molten silicon droplet is lowered intentionally at a given  $P_{\text{O}_2}$ , crossing the equilibrium condition with respect to temperature and oxygen partial pressure for formation of a  $\text{SiO}_2$  phase, the system becomes supersaturated. Surface oxidation takes place under an undercooling level of 100 K and supersaturation of over one order magnitude of  $P_{\text{O}_2}$ . The silicon melt surface is oxidized by oxygen from both the gas and the melt phases. The formation of a  $\text{SiO}_2$  phase is an exothermic reaction. Thus, the temperature rises

unless the chemical reaction takes place very slowly. On the other hand, under these conditions, the equilibrium partial pressure of SiO is so high that this results in sublimation of SiO decomposed from  $\text{SiO}_2$ :  $\text{SiO}_2$  (solid) =  $\text{SiO}$  (gas) +  $1/2\text{O}_2$  (gas). Since this reaction is endothermic, the silicon droplet is undercooled spontaneously. This abrupt temperature decrease results in supersaturation of oxygen followed by exothermic oxidation reaction. Consequently, temperature oscillation takes place.

### 3.4. Crystal growth of silicon in an atmosphere with various $P_{\text{O}_2}$

Single crystal growth of silicon was attempted in an atmosphere with various oxygen partial pressures, in

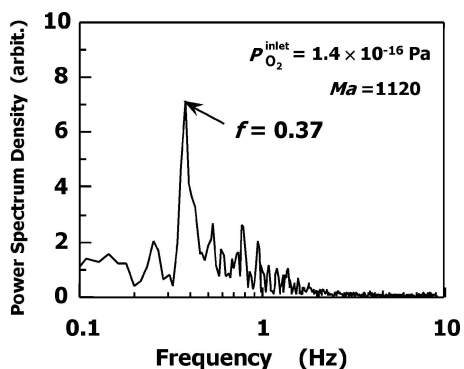


Figure 11 Frequency of growth striation for a silicon single crystal grown at  $P_{O_2}^{\text{surface}} = 1.4 \times 10^{-16}$  Pa ( $Ma = 1120$ ).

order to observe the effect of oxygen partial pressure on the formation of growth striation. Because the dimensions of the molten zone are so small, the effect of buoyancy is almost negligible.

The oxygen partial pressure of the atmosphere at the surface was controlled within a range from  $P_{O_2}^{\text{surface}} = 5.3 \times 10^{-24}$  Pa to  $3.6 \times 10^{-14}$  Pa so that the estimated temperature coefficient of surface tension according to Mukai's measurement changed from  $\partial\sigma/\partial T = -0.74$  to  $-0.22 \times 10^{-3}$  N/K-m; the corresponding Marangoni number ranged from 2000 to 616. Because the oxygen partial pressure of  $P_{O_2}^{\text{surface}} = 3.6 \times 10^{-14}$  Pa is higher than that of the equilibrium condition for the  $\text{SiO}_2$  phase formation, the surface of molten zone became coated with oxide film. This agrees with the experimental result mentioned in Section 3.3; The surface of the molten silicon droplet was oxidized at  $P_{O_2}^{\text{surface}} = 3.5 \times 10^{-14}$  Pa. This means that the temperature coefficient of  $\partial\sigma/\partial T = -0.22 \times 10^{-3}$  N/K-m and the corresponding Marangoni number of  $Ma = 616$  are not realistic, although a temperature coefficient  $\partial\sigma/\partial T$  smaller than this value has been generally reported in numerical modeling, because conventionally surface tension measurement was carried out without taking oxygen partial pressure into consideration. In such a case, the surface of the molten silicon was coated with  $\text{SiO}_2$  film. This means that measured values are surface stress and its temperature coefficient. The smallest temperature coefficient would be  $|\partial\sigma/\partial T| = |-0.25 \sim -0.30 \times 10^{-3}|$  N/K-m, where the silicon melt coexists with  $\text{SiO}_2$ .

Fig. 11 shows a result of FFT analysis of growth striation for a crystal grown at  $P_{O_2}^{\text{surface}} = 1.4 \times 10^{-16}$  Pa, i.e.  $Ma = 1120$ . Growth striation was observed for all absolute value specimens; this means that an increase in oxygen partial pressure can neither stop the flow nor suppress the formation of growth striation at  $P_{O_2} < P_{O_2}^{\text{SiO}_2}$ . Preliminary results on the observation of growth striation suggest that striation becomes intense with increasing  $P_{O_2}$ . This could be caused by increases in temperature oscillation due to strong evaporation of SiO.

#### 4. Conclusion

Marangoni flow of the molten silicon has been intensively investigated. In particular, the time dependent behavior was experimentally studied for the first time. In the future, the Marangoni flow with medium Marangoni

numbers ( $Ma = 100$ – $1000$ ) should be studied so that the time evolution of the instability mode can be understood more clearly. The effects of oxygen partial pressure on the Marangoni flow should be studied more using an ideal material, because, for the silicon case, the melt surface becomes coated with a  $\text{SiO}_2$  film before exhibiting a conversion of the sign of the temperature coefficient from negative to positive.

#### Acknowledgement

A part of the present work was carried out under the contract from Japan Space Forum and supported by the Kato Foundation.

#### References

1. A. EYER, H. LEISTE and R. NITSCHKE, in Proc. 5th European Symposium on Materials Sciences under Microgravity, Schloß Elmau 1984 (ESA SP-222) p. 173.
2. NAKAMURA, T. HIBIYA, K. KAKIMOTO, N. IMAISHI, S. NISHIZAWA, A. HIRATA, K. MUKAI, S. YODA and T. S. MORITA, *J. Cryst. Growth* **186** (1998) 85.
3. D. SCHWABE, R. VELTEN and A. SCHARMANN, *ibid.* **99** (1990) 1258.
4. S. SHIRATORI, S. YASUHIRO and T. HIBIYA, *ibid.* **266** (2004) 145.
5. R. RUPP, G. MÜLLER and G. NEUMANN, *ibid.* **97** (1989) 34.
6. M. WANSCHURA, V. SHEVTSOVA, H. C. KUHLMANN and H. J. RATH, *Phys. Fluids* **7** (1995) 912.
7. J. LEYPOLDT, H. C. KUHLMANN and H. J. RATH, *J. Fluid Mech.* **414** (2000) 285.
8. N. IMAISHI, S. YASUHIRO, Y. AKIYAMA and S. YODA, *J. Cryst. Growth* **230** (2001) 164.
9. S. YASUHIRO, N. IMAISHI, Y. AKIYAMA, S. FUJINO and S. YODA, *ibid.* **262** (2004) 631.
10. M. SCHWEIZER, A. CRÖLL, P. DOLD, TH. KAISER, M. LICHTENSTEIGER and K. W. BENZ, *ibid.* **203** (1999) 500.
11. S. NAKAMURA, T. HIBIYA, N. IMAISHI and S. YODA, *Adv. Space Res.* **24** (1999) 1417.
12. P. DOLD, M. SCHWEIZER, A. CRÖLL and K. W. BENZ, *J. Cryst. Growth* **237–239** (2002) 1671.
13. T. HIBIYA, Y. ASAI, M. SUMIJI and T. KOJIMA, *Cryst. Res. Technol.* **38** (2003) 619.
14. S. NAKAMURA, T. HIBIYA, N. IMAISHI, S. YODA, T. NAKAMURA and M. KOYAMA, *Microgr. Sci. Technol.* **12** (1999) 56.
15. T. AZAMI, S. NAKAMURA and T. HIBIYA, *J. Electrochem. Soc.* **148** (2001) G185.
16. *Idem.*, *J. Cryst. Growth* **223** (2001) 116.
17. M. SUMIJI, S. NAKAMURA, T. AZAMI and T. HIBIYA, *ibid.* **223** (2001) 503.
18. K. MUKAI, Z. YUAN, K. NOGI and T. HIBIYA, *ISIJ International* **40** (2000) S148.
19. M. RATTO, E. RICCI and E. ARATO, *J. Crystal Growth* **217** (2000) 233.
20. M. RATTO, E. RICCI, E. ARATO and P. COSTA, *Metallog. Mater. Trans. B* **32B** (2001) 903.
21. N. YAMANE, K. NAGAFUCHI, S. SHIRATORI, H. OKUBO, N. SATO and T. HIBIYA, *J. Mat. Sci.* **40** (2005).
22. N. OKUBO, R. JONO, S. SHIRATORI, S. GOTO and T. HIBIYA, HTC-2004, *ibid.* **40** (2005).
23. T. AZAMI and T. HIBIYA, *J. Cryst. Growth*, **233** (2001) 417.
24. T. HIBIYA, S. HOKAMA, Y. KOIKE, M. RINNO, H. KAWAMURA, H. FUKUYAMA, K. HIGUCHI and M. WATANABE, submitted to Scripta Materialia.

Received 31 March  
and accepted 18 July 2004